JPE 12-3-7

http://dx.doi.org/10.6113/JPE.2012.12.3.439

Input-Series Multiple-Output Auxiliary Power Supply Scheme Based on Transformer-Integration for High-Input-Voltage Applications

Tao Meng†, Hongqi Ben*, and Guo Wei*

†*School of Electrical Engineering and Automation, Harbin Institute of Technology, Harbin, China

Abstract

In this paper, an input-series auxiliary power supply scheme is proposed, which is suitable for high input voltage and multiple-output applications. The power supply scheme is based on a two-transistor forward topology, all of the series modules have a common duty ratio, all the switches are turned on and off simultaneously, and the whole circuit has a single power transformer. It does not require an additional controller but still achieves efficient input voltage sharing (IVS) for each series module through its inherent transformer-integration strategy. The IVS process of this power supply scheme is analyzed in detail and the design considerations for the related parameters are given. Finally, a 100W multiple-output auxiliary power supply prototype is built, and the experimental results verify the feasibility of the proposed scheme and the validity of the theoretical analysis.

Key words: Common duty ratio, Input series, Input voltage sharing (IVS), Magnetic integration, Multiple-output auxiliary power supply

I. INTRODUCTION

In the application of high dc voltage input, the problem of high voltage stresses imposed on the switching devices of the DC/DC converters represents a major design challenge. For example, in a three-phase power factor correction converter with a line voltage of 380VAC/50Hz, the output voltage can be as high as 760V to 1000V, in railway electrical systems, the dc supply voltage is up to 2000V to 4000V, and in the coalmining industry, the dc input voltage of the frequency converter of a miner (taking the 1140V frequency converter of a miner as an example) can be over 2000V when the motor is operating as a generator [1].

It is well known that the large voltage stress of switches is one of the bottlenecks of DC/DC converters for high voltage conversion. One of the solutions to this problem is a multi-switch series, but to achieve the voltage balancing of all of the switches, some others serious problems can not be avoided [2]-[4]. Another solution is the use of multilevel DC/DC converters. However, the number of additional clamping diodes and flying capacitors increases, and the associate control becomes more complex as the number of levels increases [5]-[7]. A third option is the use of input-series connected converters. This approach can solve the problems brought from high voltage conversion more efficiently. Input-series connected DC/DC converters can be classified into two types on the basis of the connection forms: input-series output-series (ISOS) and input-series output-parallel (ISOP). Each configuration has its own specific application areas. Generally, the ISOS converter is suitable for applications involving a high output voltage, while the ISOP converter can be used in applications where the output voltage is relatively lower [9]-[15]. Fig. 1 shows the configuration of an ISOP DC/DC converter, which includes the following advantages: 1) ease of choice of devices due to the reduced voltage stress on each module, 2) increased efficiency due to the use of low voltage MOSFETs, and 3) ease of thermal design as a results of each module handling only a part of the total power [16]-[20].

Manuscript received Dec. 10, 2011; revised Apr. 10, 2012
Recommended for publication by Associate Editor Yong-Chae Jung.
†Corresponding Author: mengtao@hit.edu.cn
Tel: +86-451-86413602, Fax: +86-451-86413602, HIT
*School of Electrical Engineering and Automation, Harbin Institute of Technolgy, China

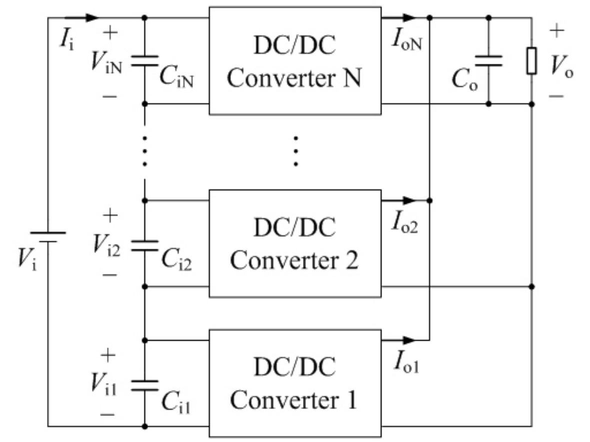

Fig. 1. ISOP DC/DC converter configuration.

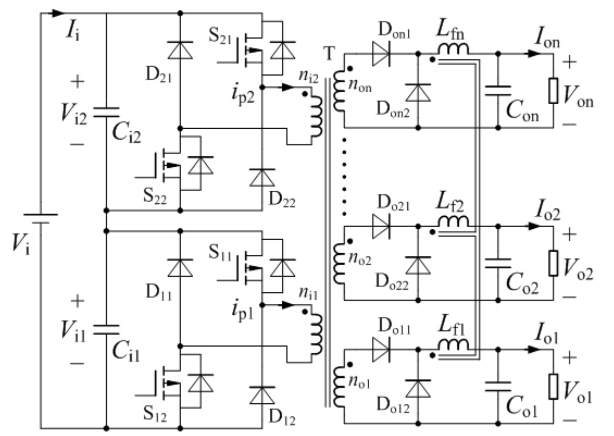

Fig. 2. Configuration of proposed input-series multiple-output auxiliary power supply.

The important issues of ISOP converters are ensuring the input voltage sharing (IVS) and the output current sharing (OCS) for each module [1], [18]. Several control schemes have been proposed to achieve these goals. In [8], a two-module ISOP system has been implemented, using a charge control technique with input voltage feed forward. In [12], [15] and [16], three-loop control schemes have been used by sensing both the input voltage and the output current. In [19], a decoupled master/slave control for an ISOP converter was proposed to deal with low cost, high voltage auxiliary power supplies. In [17], a sensor-less current mode controller was presented to guarantee stable sharing of the input voltage and the output current. In [7], [10] and [20], the uniform voltage distribution control approach was employed to realize active IVS and OCS. However, in the ISOP converters mentioned above, a dedicated IVS controller must be used, which results in increased complexity of the associated control and decreased reliability of the whole system. For auxiliary power supplies, simplicity and high-reliability of the whole system are very important. In [21], [22], a common-duty-ratio control scheme was proposed for ISOP converters. This can ensure IVS and OCS without an additional IVS or OCS controller. However, it was not suitable for multiple-output power supply systems due to the connection structure of its output side. In [23]-[25], two-module ISOP systems were investigated. In these approaches, a single transformer with two primary windings for the two-module was used, and IVS was automatically achieved due to the volt-second balance of the transformer primary windings. The number of series-modules can not be increased because of the transformer operating in bidirectional excitation mode with the two modules interleaved working.

In this paper, an input-series configuration scheme is proposed, which is suitable for multiple-output auxiliary power supplies with a high voltage input. In this configuration, all the series modules have a common duty ratio and a single power transformer. This scheme does not require any additional controllers but still achieves IVS efficiently. The IVS process of the proposed power supply scheme and the design considerations for its related parameters are given, which are then verified by experimental results.

II. The Proposed Configuration and Its Principle

A. Proposed configuration

The configuration of the proposed input-series multiple-output auxiliary power supply is shown in Fig. 2. It is based on a two-transistor forward topology. All of the modules are connected in series in the input side (to simplify the analysis, the series-module number "N"=2 is considered here), they employ the same power transformer T, and the transformer contains two identical primary windings and multiple secondary windings. The two modules share the same control circuit, and all of the switches are turned on and off simultaneously. The coupled-inductor technique is used in the output side, which can improve the output features of the multiple-output converter [26], [27].

The two modules have common output circuits, so the OCS problem has not been considered here. Theoretically, the voltage stress for each of the power devices of the two modules is $V_i/2$, and the current of each primary winding is $i_{p1}=i_{p2}$, if the turns of their windings is $n_{i1}=n_{i2}$.

B. The IVS Process

To simplify the analysis, it is assumed that: 1) all of the power devices are ideal, 2) the output can be considered as a constant current source due to the large output filter inductance, 3) the two modules have the same parameters, namely, their filter capacitors are $C_{i1}=C_{i2}=C_i$, the turns of their windings are $n_{i1}=n_{i2}=n_i$, and their equivalent leakage inductances in the primary side of T are $L_{lk1}=L_{lk2}=L_{lk}$.

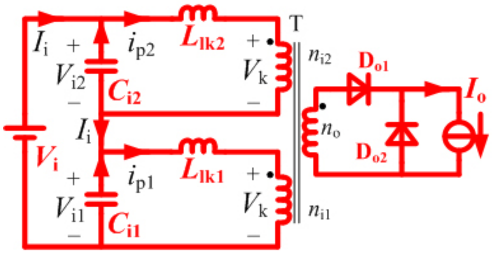

(a) Stage 1.

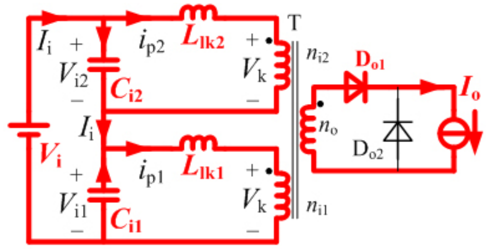

(b) Stage 2.

Fig. 3. Equivalent circuits of two stages.

The IVS process takes place during the period when all the switches are turned on. There are two stages in that period. The equivalent circuits of the two stages are shown in Fig. 3. Here the multiple output circuits are considered as a single current source I_o and the excitation inductance of the transformer is neglected. After these two simplifications, identical final results can be obtained through a simpler calculating process.

It is assumed that there is a difference between V_{i1} and V_{i2} before the switches are turned on.

$$\begin{cases} V_{i1} = \mathrm{a}V_i = V_i/2 + \Delta V_0 \\ V_{i2} = \mathrm{b}V_i = V_i/2 - \Delta V_0 \end{cases} \tag{1}$$

where, a>1/2>b, a+b=1 and $\Delta V_0 > 0$.

Stage 1 (before t_0): All of the switches are turned on. The diodes D_{o1} and D_{o2} are turning on, and the output current I_o is transferring from D_{o2} to D_{o1}. As a result, the voltage in both the primary and secondary sides of T is zero. In the primary side, L_{lk1} and L_{lk2} are charged by V_{i1} and V_{i2} respectively, and i_{p1} and i_{p2} increase rapidly. The changing of V_{i1} and V_{i2} in this stage can be ignored. At t_0, the current of D_{o1} is increased to I_o, and i_{p1} and i_{p2} can be calculated as:

$$i_{p1}(t_0) = \mathrm{a}I_o', \quad i_{p2}(t_0) = \mathrm{b}I_o' \tag{2}$$

$$I_o' = I_o n_o / n_i \tag{3}$$

Stage 2 (after t_0): The energy is transferred from the input side to the output side through the transformer T. Therefore, the following relationships can be obtained:

$$\begin{cases} i_{p1}(t-t_0) = \mathrm{a}I_o' + \int_{t_0}^{t} \dfrac{V_{i1}(t-t_0) - V_k}{L_{lk}} \mathrm{d}t \\ i_{p2}(t-t_0) = \mathrm{b}I_o' + \int_{t_0}^{t} \dfrac{V_{i2}(t-t_0) - V_k}{L_{lk}} \mathrm{d}t \end{cases} \tag{4}$$

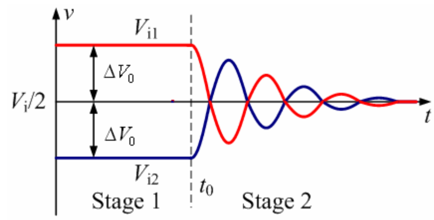

Fig. 4. Varying curves of V_{i1} and V_{i2} during stage 1and stage 2.

$$V_{i1}(t-t_0) + V_{i2}(t-t_0) = V_i \tag{5}$$

$$i_{p1}(t-t_0) + i_{p2}(t-t_0) = I_o' = 2I_i \tag{6}$$

From (4), (5) and (6), the following can be obtained:

$$V_k = V_i/2 \tag{7}$$

$$I_i = I_o'/2 \tag{8}$$

The discharging current of C_{i1} and charging current of C_{i2} can be calculated as:

$$\begin{cases} i_{C1}(t-t_0) = i_{p1}(t-t_0) - I_1 \\ i_{C2}(t-t_0) = I_1 - i_{p2}(t-t_0) \end{cases} \tag{9}$$

$$i_{C2}(t-t_0) = C_i \frac{\mathrm{d}\Delta V_{i2}(t-t_0)}{\mathrm{d}t} \tag{10}$$

where $\Delta V_{i2}(t-t_0) = V_{i2}(t-t_0) - V_{i2}(t_0)$ is the increasing value of V_{i2} after t_0.

From (4), (6), (7), (8), (9) and (10), the following differential equation is obtained:

$$\frac{\mathrm{d}^2 \Delta V_{i2}(t-t_0)}{\mathrm{d}t^2} + \frac{1}{C_i L_{lk}} \Delta V_{i2}(t-t_0) = \frac{\Delta V_0}{C_i L_{lk}} \tag{11}$$

Equation (11) has the following initial data:

$$\Delta V_{i2}(t_0) = 0 \tag{12}$$

$$i_{C2}(t_0) = \frac{I_o'}{2} - \mathrm{b}I_o' \tag{13}$$

As a result, the solution of (11) is:

$$\Delta V_{i2}(t-t_0) = \Delta V_0 \left(1 - \cos\frac{t-t_0}{\sqrt{C_i L_{lk}}}\right) + \frac{\Delta V_0}{V_i} I_o' \sqrt{C_i L_{lk}} \sin\frac{t-t_0}{\sqrt{C_i L_{lk}}} \tag{14}$$

In (14), the latter item is so small that it can be ignored when compared to the former item, so the following relationships can be approximately obtained:

$$\begin{cases} V_{i1}(t-t_0) = \dfrac{V_i}{2} + \Delta V_0 \cos\dfrac{t-t_0}{\sqrt{C_i L_{lk}}} \\ V_{i2}(t-t_0) = \dfrac{V_i}{2} - \Delta V_0 \cos\dfrac{t-t_0}{\sqrt{C_i L_{lk}}} \end{cases} \tag{15}$$

The varying curves of V_{i1} and V_{i2} during stage 1 and stage 2 are shown in Fig. 4. From (15) and Fig. 4, it can be seen that: if there is a difference between V_{i1} and V_{i2} as shown in (1), the resonances of C_{i1} and C_{i2} and L_{lk1} and L_{lk2} appear when all of the switches are turned on, and the oscillation frequency can be obtained in (16). However, the amplitude decreases in each oscillation cycle due to the resistance of each power device. Therefore, if $f_o \gg f$ (f is the switching frequency of the converter), the difference between V_{i1} and V_{i2} can be eliminated during the period when all of the switches are turned on.

$$f_o = \frac{1}{2\pi\sqrt{C_i L_{lk}}} \tag{16}$$

III. Design Considerations of the Integrated-Transformer

From the analysis in section II, it can be seen that if there is a difference between V_{i1} and V_{i2}, the converter can achieve IVS by itself. While, in section II, it is assumed that the two modules have the same parameters. Generally, the difference between V_{i1} and V_{i2} will not appear under that condition.

In this section, it is assumed that there is no difference between V_{i1} and V_{i2}, namely, $V_{i1}=V_{i2}=V_i/2$. Therefore, at t_0, the following is obtained:

$$i_{p1}(t_0) = i_{p2}(t_0) = I_o'/2 \tag{17}$$

After t_0, energy is transferred from the input side to the output side through T. An equivalent circuit model is shown in Fig. 5, where L_{m1} and L_{m2} are the excitation inductance of the two primary side of T. It can be seen that the capacitors C_{i1} and C_{i2} have a common charging current I_i and two discharging currents i_{p1} and i_{p2} which can be calculated as:

$$\begin{cases} i_{p1}(t-t_0) = \dfrac{I_o'}{2} + i_{Lm1}(t-t_0) \\ i_{p2}(t-t_0) = \dfrac{I_o'}{2} + i_{Lm2}(t-t_0) \end{cases} \tag{18}$$

From (18), it can be seen that there are two independent items i_{Lm1} and i_{Lm2} and a common item "$I_o'/2$" in the two discharging currents, and i_{p1}, i_{p2}. i_{Lm1} and i_{Lm2} can be calculated as:

$$\begin{cases} i_{Lm1}(t-t_0) = \displaystyle\int_{t_0}^{t} \frac{V_{i1}(t-t_0)}{L_{lk1}+L_{m1}} dt \\ i_{Lm2}(t-t_0) = \displaystyle\int_{t_0}^{t} \frac{V_{i2}(t-t_0)}{L_{lk2}+L_{m2}} dt \end{cases} \tag{19}$$

Here the increasing of V_{i1} and V_{i2}, caused by the two independent items of discharging current i_{Lm1} and i_{Lm2}, is considered alone. Therefore, the following relationships can be obtained:

$$\begin{cases} C_{i1}\dfrac{dV_{i1}(t-t_0)}{dt} = -i_{Lm1}(t-t_0) \\ C_{i2}\dfrac{dV_{i2}(t-t_0)}{dt} = -i_{Lm2}(t-t_0) \end{cases} \tag{20}$$

From (19) and (20), two differential equations can be obtained:

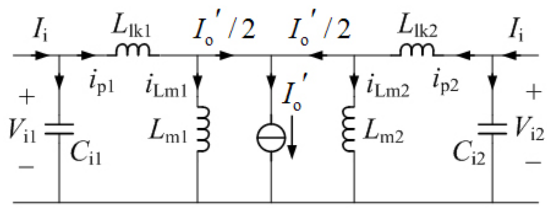

Fig. 5. Equivalent circuit model after t_0.

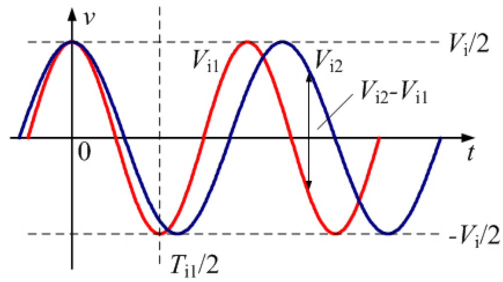

Fig. 6. Differences between V_{i1} and V_{i2}.

$$\begin{cases} \dfrac{d^2V_{i1}(t-t_0)}{dt^2} + \dfrac{1}{C_{i1}(L_{lk1}+L_{m1})}V_{i1}(t-t_0) = 0 \\ \dfrac{d^2V_{i2}(t-t_0)}{dt^2} + \dfrac{1}{C_{i2}(L_{lk2}+L_{m2})}V_{i2}(t-t_0) = 0 \end{cases} \tag{21}$$

The equations have the following initial data:

$$V_{i1}(t_0) = V_{i2}(t_0) = V_i/2 \tag{22}$$

$$i_{Lm1}(t_0) = i_{Lm2}(t_0) = 0 \tag{23}$$

As a result, the solutions of (21) are:

$$\begin{cases} V_{i1}(t-t_0) = \dfrac{V_i}{2}\cos\dfrac{t-t_0}{\sqrt{C_{i1}(L_{lk1}+L_{m1})}} \\ V_{i2}(t-t_0) = \dfrac{V_i}{2}\cos\dfrac{t-t_0}{\sqrt{C_{i2}(L_{lk2}+L_{m2})}} \end{cases} \tag{24}$$

From (24), varying curves of V_{i1} and V_{i2} can be obtained in can be seen in Fig. 6. It can be seen that that the difference between V_{i1} and V_{i2} is caused by the differences between C_{i1} and C_{i2}, L_{lk1} and L_{lk2} as well as L_{m1} and L_{m2}. The difference between two capacitors with the same capacitance is due to their tolerance feature, and it can not be improved by the designer of the power supply. For different transformers, it is nearly impossible for the inductance parameters, especially the leakage inductance, to be absolutely identical. Therefore, the difference between V_{i1} and V_{i2} can not be eliminated.

However, it can be seen from Fig. 6 that in the period 0-$T_i/2$ (T_i is the cycle of V_{i1} or V_{i2}), the difference between V_{i1} and V_{i2} is much smaller than during other periods. Here, the parameters should be designed to make sure that V_{i1} and V_{i2} can only be varying within 0-$T_i/2$. Therefore, the following relationship can be obtained:

$$\pi\sqrt{C_i(L_{lk}+L_m)} > T_{on\text{-}max} \tag{25}$$

where $T_{on\text{-}max}=D_{max}/f$ is the duration of the period when all of the switches are turning on.

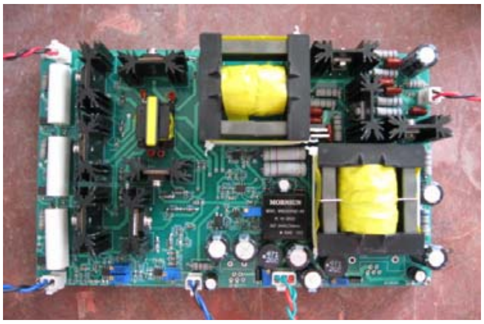

(a) Photo.

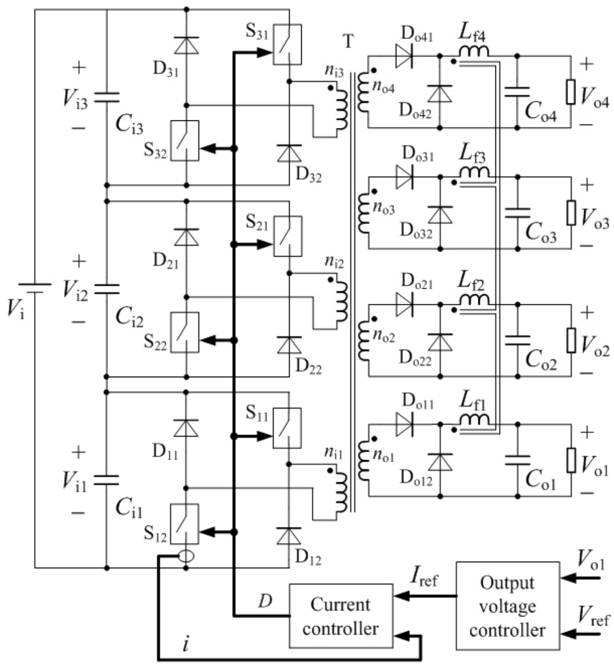

(b) Scheme.

Fig. 7. Photo and Scheme of the auxiliary power supply.

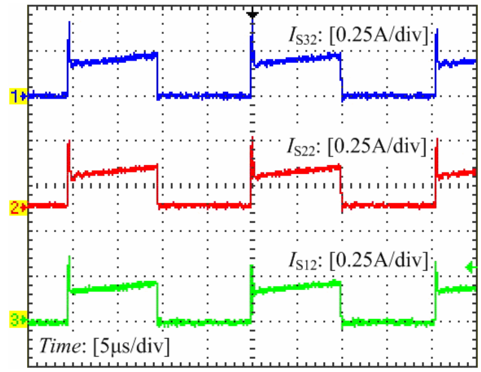

(a) When V_i=1000V.

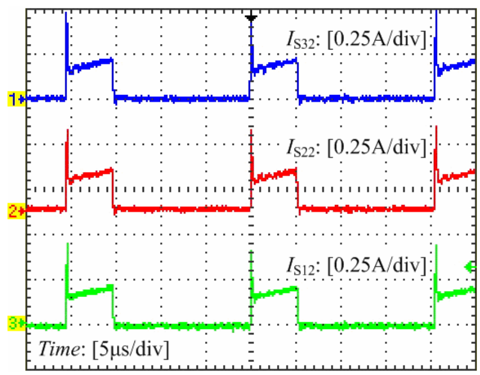

(b) When V_i is about 2098V.

Fig. 8. Current waveforms of the switches S_{12}, S_{22} and S_{32}.

Generally, $L_m \gg L_{lk}$, so (25) can be simplified as:

$$\pi\sqrt{C_i L_m} > T_{\text{on-max}} \tag{26}$$

From the analysis above, it can be concluded that the differences between V_{i1} and V_{i2} will decrease as C_i and L_m increase. However, in low power DC/DC conversion, the input filter capacitance is much smaller (generally, C_i is within 1μF). Therefore, when designing an integrated transformer, to achieve IVS more efficiently, the value of L_m can be increased properly.

IV. Experimental Verifications

A. Prototype Constructing

In order to verify the theoretical analysis in previous sections, a 100W auxiliary power supply prototype was built, as shown in Fig. 7. The prototype has three two-transistor forward circuits in the input side, namely, series-module number “N”=3.

As shown in Fig. 7 (b), module 1 is the “master” converter, module 2 and 3 are “slave” converters while output 1 is the “main” output. A single output-voltage loop generates the current reference for the inner current loop of the master converter. A peak mode current controller in the master converter generates a PWM signal with a suitable duty ratio D for the isolated driving circuits of all the switches.

All of the switches of the prototype are turned on and off simultaneously, so it is very important to obtain a group of synchronous driving signals for the switches. Here the isolated driving method based on a pulse transformer is adopted. In the driving circuits, a common pulse transformer with one input winding and six identical output windings is used, through which six synchronous driving signals will be generated without any delay.

The design specifications of the prototype, its basic circuit parameters and the main utilized components’ type are as follows:

1) Input voltage: 1000-2200Vdc;

2) Output voltage and current: V_{o1}=V_{o2}=V_{o3}=V_{o4}=24Vdc, I_{o1}=1.5A, I_{o2}=I_{o3}=1A, and I_{o4}=0.5A;

3) Switching frequency f: 50kHz;

4) C_{i1}=C_{i2}=C_{i3}=0.1μF (1200V);

5) Switches S_{11}, S_{12}, S_{21}, S_{22}, S_{31} and S_{32}: K1271 (NEC);

6) Diodes D_{11}, D_{12}, D_{21}, D_{22}, D_{31} and D_{32}: BYV26G (Philips);

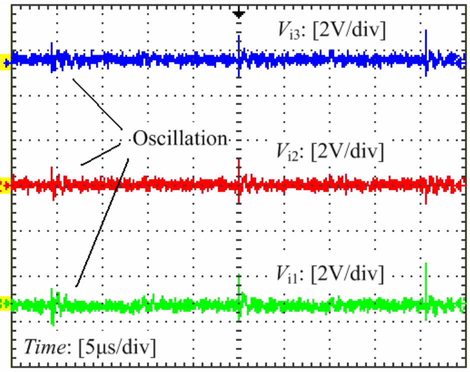

(a) When V_i=1000V.

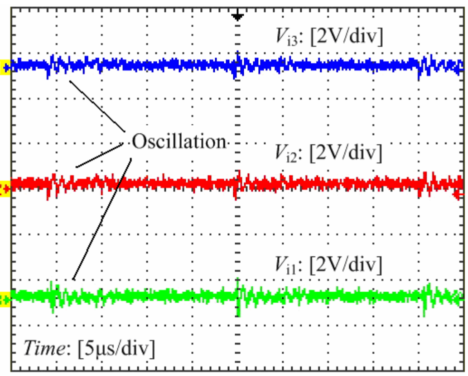

(b) When V_i is about 2098V.

Fig. 9. Input voltage waveform of each module (ac coupling).

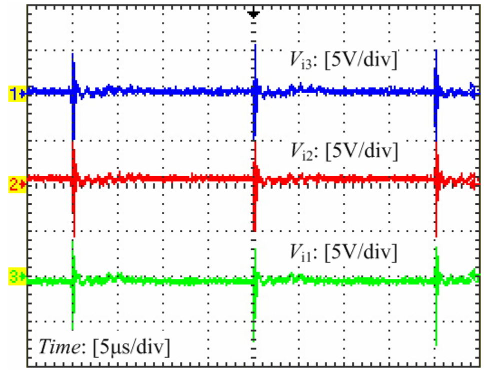

(a) Input voltage waveform of each module (ac coupling).

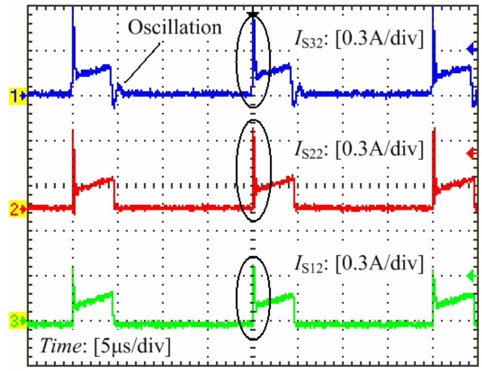

(b) Current waveforms of the switches S_{12}, S_{22} and S_{32}.

Fig. 10. Experimental results with T_a when V_i=2098V.

TABLE I
EXPERIMENTAL DATA AT FULL LOAD

V_i/kV	1.0	1.2	1.4	1.6	1.8	2.0	About 2.098
V_{i1}/V	333	399	466	532	599	665	698
V_{i2}/V	333	400	468	533	599	668	700
V_{i3}/V	334	401	467	535	602	667	701
η/%	86.2	86.5	85.1	83.7	82.2	80.6	79.2

7) Power transformer: L_m=25.6mH, L_{lk}=39μH (Ferroxcube, ETD 49, n_{i1}=n_{i2}=n_{i3}=76 turns, n_{o1}=n_{o2}=n_{o3}=n_{o4}=12 turns);

8) Rectifier diodes D_{o11}, D_{o12}, D_{o21}, D_{o22}, D_{o31}, D_{o32}, D_{o41} and D_{o42}: MUR1520 (Onsemi);

9) Coupled-inductor: L_{f1}=L_{f2}=L_{f3}=L_{f4}=1.1mH (Ferroxcube, ETD 49, 58 turns);

10) C_{o1}=C_{o2}=C_{o3}=1000μF, C_{o4}=680μF.

B. Experimental Results

The prototype scheme was designed with the aim of being used in the 1140V frequency converter of a miner as an auxiliary power supply. Therefore, the high input voltage of the prototype was obtained from the DC bus of a 1140V frequency converter of a miner, the voltage of which would be over 2000V when the motor is operating in generating mode. Some proper power resistors were considered as the load of this prototype.

Fig. 8, 9 and Table I show the experimental results of the prototype operating in the steady state under a full load. Fig. 8 shows the current waveforms of the switches S_{12}, S_{22} and S_{32}, when V_i=1000V and V_i is about 2098V. The current spike of each waveform is brought from the reverse recovery process of the rectifier diodes: D_{o12}, D_{o22}, D_{o32} and D_{o42}, when all of the switches are turned on. From Fig. 8, it can be seen that there are nearly no differences among the three current waveforms, which proves that all of the switches can be turned on and off simultaneously. Fig. 9 shows the waveforms of V_{i1}, V_{i2} and V_{i3}, when V_i=1000V and V_i is about 2098V. It can be seen that the voltage oscillation caused by the resonance among the three modules is very small and that the prototype has a high reliability. From Table I, it can be seen that the differences among the input voltage of each of the modules are very small and that the IVS has been achieved efficiently in this prototype. The efficiency of this prototype is slightly lower than that of the conventional two-transistor forward circuit with a wide range input voltage. However, its efficiency is relatively higher when the input voltage is near the rated value of 1140V, and the maximum efficiency is higher than 86%.

From the analysis in section III, it can be seen that the IVS can be achieved more efficiently as the value of L_m increases. Therefore, to verify the analysis, another power transformer

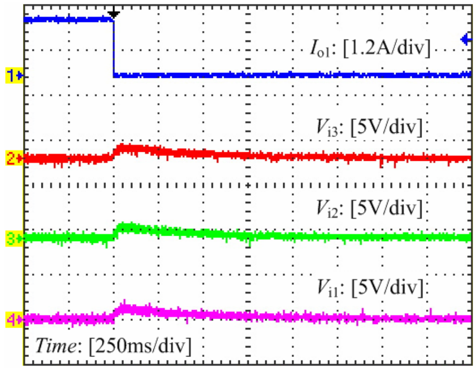

(a) Step down.

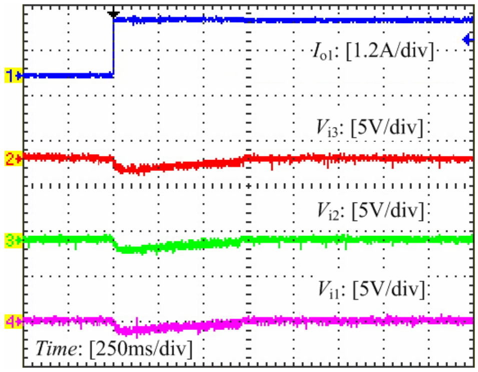

(b) Step up.

Fig. 11. Response in individual input voltage of each module (ac coupling) to a stepped load of the main output when V_i is about 1600V.

T_a (Ferroxcube, EI 50, L_m=5.9mH, L_{lk}=6μH, n_{i1}=n_{i2}=n_{i3}=38 turns, n_{o1}=n_{o2}=n_{o3}=n_{o4}=6 turns) has been made. Compared with T (Ferroxcube, ETD49, L_m=25.6mH, L_{lk}=39μH, n_{i1}=n_{i2}=n_{i3}=76 turns, n_{o1}=n_{o2}=n_{o3}=n_{o4}=12 turns), the turn ratio has not been changed, while the excitation inductance L_m and the leakage inductance L_{lk} are much smaller. Fig. 10 shows the experimental results when T_a is used and V_i is about 2098V (because the excitation inductance is much smaller than that of T, to avoid the saturation of T_a, the prototype can not operate under a full load). Compared to the experimental results in Fig. 9 (b), it can be seen, from Fig. 10 (a), that the oscillation among the input voltage of each of the modules become much higher, its frequency increases and the IVS of this prototype is achieved less efficiently. This verifies the analysis in section III and expression (15). From Fig. 10 (b), a more obvious difference among each of the current waveforms can be seen. This is caused by the more serious voltage oscillation here.

Fig. 11 shows the individual input voltage of each of the modules corresponding to a load stepping of the main output between full load (1.5A) and standby load (about 0.1A), when V_i is about 1600V. Because there is a bulk capacitor connected in parallel with the DC bus of the frequency converter, the total input voltage V_i will change slightly and

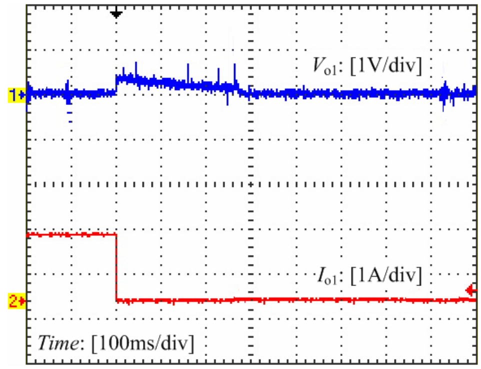

(a) Step down.

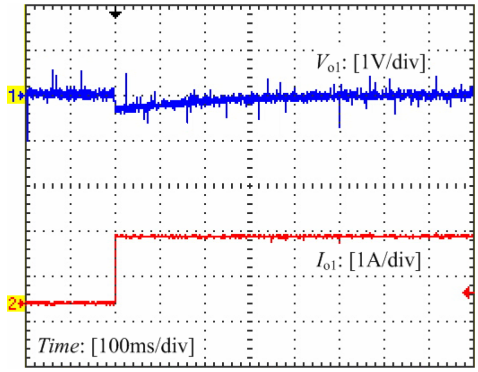

(b) Step up.

Fig. 12. Response in the main output voltage (ac coupling) to a step change of its load current when V_i is about 1600V.

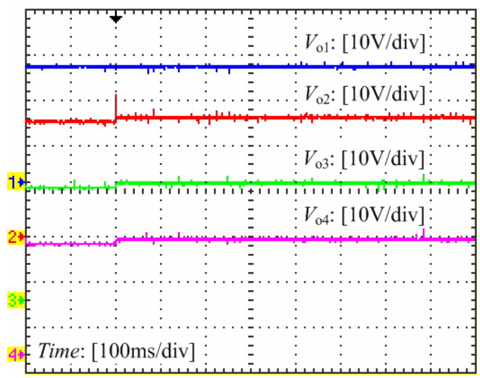

(a) Step down.

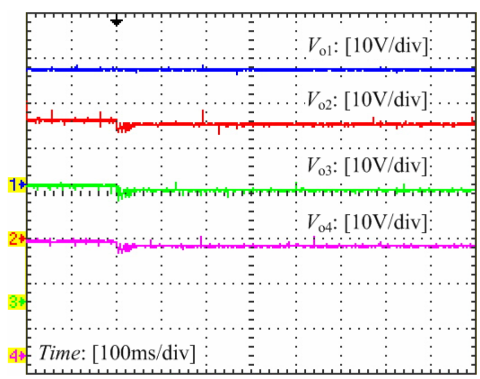

(b) Step up.

Fig. 13. Response of the four output voltage to a stepped load of the main output when V_i is about 1600V.

slowly with the load stepping. It can be seen that despite the transients, the changes of V_{i1}, V_{i2} and V_{i3} are synchronous, and there is no influence on the IVS of the prototype.

Fig. 12 and 13 show the deviations in each of the output voltages corresponding to a load stepping of the main output between full load and standby load, when V_i is about 1600V. As seen in Fig. 12, an exponential response and a peak pulse of less than 1.8% demonstrate that the scheme in this paper does not adversely affect the stability or the performance of the output-voltage-control loop. From Fig. 13, it can be seen that an identical coupled-inductor technique in a conventional multiple-output circuit is also suitable in this prototype to improve the multiple-output voltage cross-regulation feature.

V. Conclusions

An input-series multiple-output auxiliary power supply scheme is proposed and investigated in this paper which is mainly used for high voltage input and multiple-output applications. The theoretical analysis shows that the power supply can achieve IVS relying on its inherent transformer-integration strategy. Its IVS effect can be influenced by the input filter capacitor and the excitation inductance of each of the series-modules. Finally, following the design procedure, a 100W power supply prototype with a high voltage input is built. Experimental results are obtained from the prototype with two different integrated transformers respectively, which verifies the method and the analysis in this paper.

Acknowledgment

This work was supported by the National Natural Science Foundation of China under Grant No. 51107017. Thanks for the help of Liaotong Electric of Co., Ltd.

References

[1] T. Fang, X. Ruan, and C. K. Tse, "Control strategy to achieve input and output voltage sharing for input-series-output-series-connected inverter systems," *IEEE Trans. Power Electron.*, Vol. 25, No. 6, pp. 1585-1596, Jun. 2010.

[2] C. Gerster, "Fast high-power/high-voltage switch using series-connected IGBT's with active gate-controlled voltage-balancing," in *Proc. IEEE APEC*, pp. 469-472, 1994.

[3] A. Consoli, S. Musumeci, G. Oriti and A. Testa, "Active voltage balancement of series connected IGBTs," in *Proc. IEEE IAS*, pp. 2752-2758, 1995.

[4] C. Gerster, P. Hofer and N. Karrer, "Gate-control strategies for snubberless operation of series connected IGBTs," in *Proc. IEEE PESC*, pp. 1739-1742, 1996.

[5] G. Gateau, M. Fadel, P. Maussion, R. Bensaid and T. Meynard, "Multicell converters: active control and observation of flying-capacitor voltages," *IEEE Trans. Ind. Electron.*, Vol. 49, No. 5, pp. 998-1008, Oct. 2002.

[6] M. Yamamoto, S. Sato, E. Hiraki and M. Nakaoka. "Auxiliary resonant commutated leg snubber linked 3-level 3-phase voltage source soft-switching inverter," *Journal of Power Electronics*, Vol. 3, No. 2, pp: 90-98, Jul. 2003.

[7] X. Ruan, W. Chen, L. Cheng, C. K. Tse and T. Zhang, "Control strategy for input-series-output-parallel converters," *IEEE Trans. Ind. Electron.*, Vol. 56, No. 4, pp. 1174-1185, Apr. 2009.

[8] J. W. Kim, J. S. You and B. H. Cho, "Modeling, control, and design of input-series-output parallel-connected converter for high-speed-train power system," *IEEE Trans. Ind. Electron.*, Vol. 48, No. 3, pp. 536-544, Jun. 2001.

[9] S. P. Natatarajan and T. S. Anandhi. "Control of input series output parallel connected DC-DC converters," *Journal of Power Electronics*, Vol. 7, No. 3, pp: 265-270, Jul. 2007.

[10] W. Chen, X. Ruan, H. Yan and C. K. Tse, "DC/DC conversion systems consisting of multiple converter modules: stability, control, and experimental verifications," *IEEE Trans. Power Electron.*, Vol. 24, No. 6, pp. 1463-1474, Jun. 2009.

[11] Y. Huang, C. K. Tse and X. Ruan, "General control considerations for input-series connected DC/DC converters," *IEEE Trans. Circuits Syst. I, Reg. Papers*, Vol. 56, No. 6, pp. 1286-1386, Jun. 2009.

[12] W. Chen, K. Zhuang and X. Ruan, "A input-series- and output-parallel connected inverter system for high-input-voltage applications," *IEEE Trans. Power Electron.*, Vol. 24, No. 9, pp. 2127-2137, Sep. 2009.

[13] J. P. Lee, B. D. Min, T. J. Kim, D. W. Yoo and J. Y. Yoo. "Input-series-output-parallel connected DC/DC converter for a photovoltaic PCS with high efficiency under a wide load range," *Journal of Power Electronics*, Vol. 10, No. 1, pp: 9-13, Jan. 2010.

[14] D. S. Sha, Z. Q. Guo and X. Z. Liao, "Digital control strategy for input-series-output-parallel modular DC/DC converters," *Journal of Power Electronics*, Vol. 10, No. 3, pp: 245-250, May. 2010.

[15] A. Bhinge, N. Mohan, R. Giri and R. Ayyanar, "Series-parallel connection of DC-DC converter modules with active sharing of input voltage and load current," in *Proc. IEEE APEC*, pp. 648-653, 2002.

[16] R. Ayyanar, R. Giri and N. Mohan, "Active input-voltage and load-current sharing in input-series and output-parallel connected modular DC-DC converters using dynamic input-voltage reference scheme," *IEEE Trans. Power Electron.*, Vol. 19, No. 6, pp. 1462-1473, Nov. 2004.

[17] J. W. Kimball, J. T. Mossoba and P. T. Krein, "A stabilizing, high-performance controller for input series-output parallel converters," *IEEE Trans. Power Electron.*, Vol. 23, No. 3, pp. 1416-1427, May. 2008.

[18] D. Sha, Z. Guo and X. Liao, "Cross-feedback output-current-sharing control for input-series-output parallel modular DC-DC converters," *IEEE Trans. Power Electron.*, Vol. 25, No. 11, pp. 276-2771, Nov. 2010.

[19] P. J. Grbovic, "Master/slave control of input-series- and output-parallel connected converters: concept for low-cost high-voltage auxiliary power supplies," *IEEE Trans. Power Electron.*, Vol. 24, No. 2, pp. 316-328, Feb. 2009.

[20] K. Siri, M. Willhoff and K. Conner, "Uniform voltage distribution control for series connected DC-DC converters," *IEEE Trans. Power Electron.*, Vol. 22, No. 4, pp. 1269-1279, Jul. 2007.

[21] R. Giri, R. Ayyanar and N. Mohan, "Common duty ratio

control of input series connected modular DC-DC converters with active input voltage and load-current sharing," in *Proc. IEEE APEC*, pp. 322-326, 2003.
[22] R. Giri, V. Choudhary, R. Ayyanar and N. Mohan, "Common-duty-ratio control of input-series connected modular DC-DC converters with active input voltage and load-current sharing," *IEEE Trans. Ind. Appl.*, Vol. 42, No. 4, pp. 1101-1111, July./Aug. 2006.
[23] R. Torrico-Bascope and I. Barbi, "A double ZVS-PWM active-clamping forward converter: analysis, design, and experimentation," *IEEE Trans. Power Electron.*, Vol. 16, No. 6, pp. 745-751, Nov. 2001.
[24] D. V. Ghodke and K. Muralikrishnan, "Zvzcs, dual, two-transistor forward DC-DC converter with peak voltage of Vin/2, high input and high power application," in *Proc. IEEE APEC*, pp. 1853-1858, 2002.
[25] X. Ma, W. Wang, Y. Kang and J. Chen, "Series of two transistors forward ZVZCS converter with phase-shifted control for high input voltage," in *Proc. IEEE IECON*, pp. 761-766, 2004.
[26] D. Maksimovic, R. W. Erickson and C. Griesbach, "Modeling of cross-regulation in converters containing coupled inductors," *IEEE Trans. Power Electron.*, Vol. 15, No. 4, pp. 607-615, Jul. 2000.
[27] J. J. Lee and B. H. Kwon, "DC-DC converter using a multiple-coupled inductor for low output voltages," *IEEE Trans. Ind. Electron.*, Vol. 54, No. 1, pp. 467-478, Feb. 2007.

Tao Meng was born in Liaoning Province, China, in 1980. He received his B.S., M.S. and Ph.D. in Electrical Engineering from the Harbin Institute of Technology, Harbin, China, in 2003, 2005 and 2010, respectively. Since 2007, he has been an Engineer with the School of Electrical Engineering and Automation, Harbin Institute of Technology. His current research interests include active power factor correction techniques, high frequency AC/DC, DC/DC power conversion techniques, magnetic integration techniques and their application.

Hongqi Ben was born in Heilongjiang Province, China, in 1965. He received his B.S. in Electrical Engineering from the Shenyang University of Technology, Shenyang, China, in 1988, his M.S. in Electrical Engineering from the Harbin Institute of Technology, Harbin, China, in 1991, and his Ph.D. in Mechatronics Engineering from the Harbin Institute of Technology, Harbin, China, in 1999. Since 2004, he has been a Professor with the School of Electrical Engineering and Automation, Harbin Institute of Technology. His current research interests include high frequency power conversion techniques and active power factor correction techniques.

Guo Wei was born in Liaoning Province, China, in 1966. He received his B.S. and M.S. in Electromagnetic Measurement and Instrument from the Harbin Institute of Technology, Harbin, China, in 1988 and 1991, respectively, and his Ph.D. in Scientific Research from Saga University, Saga, Japan, in 2003. Since 2008, he has been a Professor with the School of Electrical Engineering and Automation, Harbin Institute of Technology. His current research interests include modern sensor techniques and signal processing, intelligent testing theory and its application, and weak signal detection and processing.